ELSEVIER

Journal of Molecular Structure: THEOCHEM 810 (2007) 31–37

THEO CHEM

www.elsevier.com/locate/theochem

A comparative study on the nature and strength of O–O, S–S, and Se–Se bond

Damanjit Kaur *, Punita Sharma, Prasad V. Bharatam [1]

Department of Chemistry, Guru Nanak Dev University, Amritsar 143005, India

Received 12 December 2006; received in revised form 27 January 2007; accepted 30 January 2007
Available online 6 February 2007

Abstract

A computational study on dichalcogenide molecules (R_2X_2; X = O, S, Se; R = H, CH_3, NH_2) has been carried out employing B3LYP and MP2 levels using 6-31+G*, 6-311+G*, 6-311++G**, and PVDZ basis sets. The relative energies have been evaluated at G2MP2 also. The rotational barriers and bond dissociation energies indicate that S–S bond is stronger than Se–Se and O–O bond. NBO analysis at MP2/6-31+G* suggest the presence of partial π character between X–X bond that decreases in the order S–S > Se–Se > O–O. Fuki functions for nucleophilic and electrophilic attack fail to distinguish the reactivity of S and Se. The proton affinities of the O_2H_2, S_2H_2, Se_2H_2 decrease in the order Se > S > O.

Keywords: Diselenides; Disulfides; Rotational barrier; BDE; NBO analysis

1. Introduction

The chalcogen elements oxygen, sulfur, and selenium are the constituents of functional groups in biomolecules fulfilling a variety of important biological functions. The electronic structure of valence shell (s^2p^4) makes these elements redox active [1]. Oxygen occurs in just a few oxidation states between 0 (molecular oxygen) and −2 (water). In contrast sulfur and selenium are present in oxidation states ranging from −2 to +6 [2,3]. It is interesting to note that H_2O_2 is a well-known oxidizing agent while H_2Se_2 acts as antioxidant [4]. In aerobic organisms, during the reduction of oxygen by electron transfer systems of mitochondria, small amounts of O_2H_2, O_2, and $HO^{\cdot}$ are generated.

Structural damage to bimolecules of a wide variety (DNA, proteins, carbohydrates, and lipids) is a consequence of oxidation reactions of these species collectively named as oxidative stress [5,6]. Oxidative stress is associated with many human diseases ranging from neurodegenerative and auto inflammatory conditions such as Alzheimer's disease [7], rheumatoid arthritis, diabetes, and cancer [8]. The defense mechanism of mammalian cells involves reducing action of glutathione on H_2O_2 with the formation of H_2O and disulfide [9].

Selenoprotein enzyme glutathione peroxidase (GPx) catalyses the reduction of H_2O_2 by glutathione. There have been many attempts to mimic GPx activity with model systems such as diselenides [10]. Organic diselenides play important role in organic synthesis as well because these are stable and reactive enough to produce electrophilic and nucleophilic reagents [11]. In addition to the formation of disulfide bonds during redox action of GSH on H_2O_2, disulfides are frequently found as integral part of proteins and enzymes [12]. The disulfide bonds between cysteines stabilize the folded conformation of proteins [13].

The disulfide/thiol redox system is reported to control numerous important events in cellular life such as regulation of cell growth, proliferation [14,15] and human cancer development [16,17]. Biological and physiological effects of garlic oil are due to the presence of diallyl disulfides [18].

* Corresponding author. Tel.: +91 183 2256619.
E-mail address: damanjit32@yahoo.co.in (D. Kaur).
[1] Present address: Department of Medicinal Chemistry, National Institute of Pharmaceutical Education and research (NIPER), S.A.S. Nagar (Mohali), Punjab 160062, India.

0166-1280/$ - see front matter © 2007 Elsevier B.V. All rights reserved.
doi:10.1016/j.theochem.2007.01.038

Peroxides, disulfides, and diselenides can be together grouped as dichalcogenides yet they differ remarkably in their properties. Understanding the nature of dichalcogenide bonds for their strength and reactivity and analyzing factors responsible for their varying properties is the aim of present study. For this purpose, dihydrogen dichalcogenides and their symmetrical methyl and amino derivatives (R_2X_2; X = O, S, Se; R = H, CH_3, NH_2) have been selected.

2. Computational details

Ab initio MO [19] and density functional (DFT) [20] calculations have been performed using GAUSSIAN 98W package, the windows version of GAUSSIAN 98 suite of programs [21]. Complete optimizations have been carried out on dihydrogen diselenide, dihydrogen disulphide, hydrogen peroxide, and their methyl and amino substituted derivatives at B3LYP and MP2 levels using 6-31+G*, 6-311+G*, 6-311++G**, and PVDZ basis sets. Frequencies were computed for all the optimized structures at HF and B3LYP level using 6-31+G*, 6-311+G*, 6-311++G**, and PVDZ basis set in order to characterize each stationary point as a minimum or a transition state and to determine ZPE values. The calculations have been done at G2MP2 level to get accurate relative energies. The X–X (X = O, S, Se) rotational barriers and bond dissociation energy (BDE) have been calculated at all these levels.

BDE is calculated as the enthalpy change of the following reaction in the gas phase at 298 K and 1 atm pressure.

$$A\text{–}A(g) \rightarrow A^{\cdot}(g) + A^{\cdot}(g)$$

The bond dissociation energy is defined as the sum of heat of formation ($H^{\circ}_{f,298}$) of the products (radicals) minus those of reactants (parent molecule) [22–24].

$$BDE = \Delta H_{298} = H_f(RX^{\cdot}) + H_f(RX^{\cdot}) - H_f(RXXR)$$

The enthalpy of formation of all the species is calculated using the following equation [25–27]

$$H_{298} = E_e + ZPE + H_{trans} + H_{rot} + H_{vib} + RT$$

where E_e is electronic energy, ZPE is zero point vibrational energy [28], H_{trans} is translational enthalpy of molecules, H_{rot} is rotational enthalpy of molecule, H_{vib} is vibrational enthalpy of molecule [29,30], and RT (PV work term) is conversion factor from energy to enthalpy.

The thermal contribution to enthalpy is particularly sensitive to low frequency vibrations. Hence, two scale factors are used; one for the ZPE and other one for the vibrational contribution to enthalpy [29,31,32]. The ZPE values have been scaled by a factor of 0.9153 at HF/6-31+G*, 0.9242 at HF/6-311+G*, and HF/6-311++G**, 0.9232 at HF/PVDZ, 0.9806 at B3LYP/6-31+G*, 0.9877 at B3LYP/6-311+G*, and 6-311++G**, 0.9787 at B3LYP/PVDZ level. The Vibrational contribution to enthalpy has been scaled by a factor of 0.8951 at HF/6-311+G*, and 6-311++G**, 0.9110 at HF/PVDZ, 0.9679 at B3LYP/6-311+G*, and 6-311++G**, 0.9698 at B3LYP/PVDZ level. To apply ZPE and enthalpy correction at MP2 energies, the values obtained at HF level have been used. NBO analysis has been carried out in order to understand second order interactions [33]. In order to understand the GPx like activity of diselenides [34–37], free energy change has been evaluated for various reaction steps of catalytic cycle at B3LYP/6-311++G level.

3. Results and discussion

Since the aim of present study is to understand nature, strength, and reactivity of dichalcogenide compounds, (for chalcogens = O, S, Se) hydrogen dichalcogenides and their methyl and amino substituted derivatives are selected as model compounds. The geometrical parameters at MP2/6-311++G** and B3LYP/6-311++G** level along with experimental data [38,39] wherever available are included in Table 1. The geometrical parameters at B3LYP and MP2 levels employing 6-31+G*, 6-311+G*, and PVDZ basis sets are available in supporting information (Tables S1–3). As can be seen from Table 1, the theoretically evaluated parameters are in good agreement with the experimental results. Slight variations are the result of absence of environmental interactions in the theoretical calculations. The X–X and X–R (X = O, S, Se, R = H, CH_3, NH_2) bond distances increase in the order O < S < Se that is in accordance with increasing size and decreasing electronegativity of the chalcogen atom.

The H–X–X–H dihedral in X = S or Se is nearly 90° in comparison to 120° for X = O. The strong hydrogen bond interactions between nonbonded O and H atoms indicated by nonbonded O–H separation of 1.870 Å at MP2/6-311++G** level are responsible for the difference in the dihedral angle in dichalcogenides in the three cases. In case of X = S or Se with smaller electronegativity difference between X and H and larger size of chalcogen, such interactions become insignificant and hence lone-pair lone-pair and bond-pair bond-pair repulsive interactions decide the dihedral angle.

The S–S and Se–Se bond lengths are compressed with the presence of R = CH_3 or NH_2 while O–O bond length elongates with R = CH_3. The O–O bond length with R = NH_2 elongates to nearly nonbonded distance. The Y–O–O–Y (Y = first atom of the substituent) dihedral changes to 180.0° with R = CH_3 from 120.0° in case of R = H. The larger variation in Y–X–X–Y dihedral in substituted dichalcogenides relative to their unsubstituted counterparts in X = O in comparison to X = S or Se indicates the difference in electronic structure of the three different chalcogenides. The opposite trend in variation of X–X bond distance with the presence of substituents also indicate the same.

The rotational barriers are important indicators for the electronic structures. The steric interactions and the breaking of π-bond character wherever present are the dominant factors responsible for the rotational barriers. The rota-

Table 1
Geometrical parameters[a] of dichalcogenides {chalcogen = [O], (S), Se} at MP2/6-311++G** and *B3LYP/6-311++G*** level

Molecule	Parameters	GS X = Se, (S), [O]	TS1 X = Se, (S), [O]	TS2 X = Se, (S), [O]
X_2H_2	X–X	2.355 (2.083) [1.450] *2.370* (*2.113*) [*1.454*] (2.055)[b]	2.409 (2.136) [1.458] *2.430* (*2.174*) [*1.462*]	2.399 (2.125) [1.459] *2.418* (*2.161*) [*1.463*]
	X–H	1.463 (1.336) [0.964] *1.476* (*1.352*) [*0.967*] (1.327)[b]	1.46 (1.333) [0.965] *1.471* (*1.348*) [*0.967*]	1.461 (1.334) [0.964] *1.473* (*1.348*) [*0.966*]
	H–X–X–H	90 .67 (90.89) [121.51] *90.5* (*91.1*) [*121.3*] (90.5)[b]	−0.02 (−0.09) [−0.054] *0.0* (*0.0*) [*0.0*]	179.9 (179.9) [179.9] *179.9* (*179.9*)[*180.1*]
$X_2(CH_3)_2$	X–X	2.339 (2.065) [1.463] *2.355* (*2.091*) [*1.467*] (2.038)[c]	2.410 (2.138) [1.482] *2.435* (*2.178*) [*1.489*]	2.385 (2.111) [1.466] *2.409* (*2.148*) [*1.470*]
	X–C	1.959 (1.807) [1.414] *1.981* (*1.833*)[*1.413*] (1.810)[c]	1.953 (1.802) [1.414] *1.970* (*1.823*) [*1.413*]	1.954 (1.803) [1.413] *1.970* (*1.824*) [*1.413*]
	CH_3–X–X–CH_3	−84.84 (82.49) [180.22] *−88.2* (*−87.8*) [*−180.0*] (84.7)[b]	0.02 (−0.85) [−0.01] *0.0* (*−0.0*) [*−0.0*]	180.1 (179.9) [179.9] *180.0* (*180.0*) [*180.0*]
$X_2(NH_2)_2$	X–X	2.356 (2.054) *2.351* (*2.101*)	2.494 (2.245) *2.543* (*2.314*)	2.408 (2.150) *2.451* (*2.230*)
	X–N	1.869 (1.705) *1.876* (*1.712*)	1.825 (1.664) *1.825* (*1.669*)	1.862 (1.693) *1.862* (*1.685*)
	NH_2–X–X–NH_2	−84.7 (83.3) *−86.1*(*84.4*)	0.0 (−0.0) *0.1* (*−0.0*)	180.1 (179.9) *180.0* (*180.0*)

The bond distances are in Å and bond angles are in degrees.
[a] Values in italics are at B3LYP/6-311++G** theoretical level.
[b] Experimental values from Ref. [38].
[c] Experimental values from Ref. [39].

tions that involve the breaking of intramolecular attractive interactions enhance the rotational barriers. Two rotational transition states for X–X rotation have been optimized. The TS1 has eclipsed orientation of lone pairs and bond pairs while TS2 have staggered orientation of bond pairs and lone pairs attached to two X atoms. The X–X rotational barriers for dichalcogenides are listed in Table 2. As can be seen from the table, the barrier to

Table 2
Rotational barriers (ZPE corrected values in kcal/mol) of dichalcogenides {chalcogen = [O], (S), Se} at B3LYP (MP2) level using 6-31+G*, 6-311+G*, 6-311++G**, and PVDZ basis set and at G2MP2 level

Molecule	Transition state	6-31+G*	6-311+G*	6-311++G**	PVDZ	G2MP2
Se_2H_2	TS1	6.63 (6.67)	6.33 (6.45)	6.00 (6.29)	5.87	5.96
	TS2	4.99 (4.77)	4.74 (4.63)	4.46 (4.51)	4.46	4.36
$Se_2(CH_3)_2$	TS1	9.53 (10.03)	8.85 (9.21)	8.85 (9.10)	8.63	8.88
	TS2	5.35 (5.34)	5.39 (5.21)	5.42 (5.34)	5.44	5.30
$Se_2(NH_2)_2$	TS1	9.19 (9.97)	8.66 (9.46)	8.75 (9.91)	9.38	10.25
	TS2	6.74 (6.53)	6.07 (5.86)	6.30 (6.22)	6.68	6.77
S_2H_2	TS1	7.40 (7.89)	7.23 (7.62)	6.82 (7.25)	6.77 (7.22)	7.27
	TS2	4.80 (5.04)	4.68 (4.91)	4.44 (4.71)	4.80 (4.93)	5.08
$S_2(CH_3)_2$	TS1	10.72 (12.04)	10.41 (12.08)	10.36 (12.10)	9.97 (10.64)	11.26
	TS2	5.53 (6.01)	5.34 (6.06)	5.34 (6.23)	5.35 (5.80)	5.82
$S_2(NH_2)_2$	TS1	7.20 (9.53)	6.11(8.01)	6.25 (8.27)	7.02 (8.26)	8.96
	TS2	6.91 (7.60)	6.03 (6.79)	6.25 (7.18)	7.09 (7.64)	8.39
O_2H_2	TS1	8.48 (9.14)	9.19 (9.85)	7.89 (8.40)	6.74 (7.11)	6.84
	TS2	0.40 (0.30)	0.28 (0.27)	0.31 (0.46)	0.55 (0.63)	0.73
$O_2(CH_3)_2$	TS1	11.62 (13.06)	11.69 (13.19)	11.59 (12.76)	10.65 (11.25)	11.39
	TS2	2.57 (2.76)	2.55 (2.84)	2.47 (2.77)	2.44 (2.73)	2.63

rotation through TS2 are shorter than for rotation through TS1. The barriers are considerably larger than the C–C single bond rotational barrier for ethane which is 2.40 at B3LYP/6-311++G** level. The rotational barrier for H_2O_2, H_2S_2, and H_2Se_2 decrease in the order $H_2S_2 > H_2Se_2 > H_2O_2$ for rotation through TS2. The calculations have been done at G2MP2 level to have accurate evaluation of the barriers. Since G2MP2 results are known to be accurate within ±1 kcal/mol of the observed values, the comparison of rotational barriers with the barriers at G2MP2 level indicate that limited accuracy can be gained by adding polarization and diffuse functions to 6-31+G* basis set. The rotational barrier for dimethyl dichalcogenides for rotation through TS1 are higher than that for C–C rotational barrier (5.80 kcal/mol at B3LYP/6-311++G** level) in *n*-butane through transition state with eclipsed methyl group in spite of the fact that X–X bond lengths in dichalcogenides are longer than the C–C bond length. The longer bond length is expected to decrease the repulsive interactions between the bonding/lone pairs present on neighbouring atoms. This difference suggests that some partial π bond character between X–X bonds is present. The order of π character is best indicated by the rotational barriers for H_2X_2 for rotation through TS2 as repulsive interactions between substituent groups are not included here.

The NBO analysis has been carried out to understand whether it is only the repulsive interactions involving the lone pairs and bond pairs responsible for the relatively higher rotational barriers or there are electron delocalizations from the lone pairs present on X or the substituents. The important second order interaction energies evaluated at MP2/6-31+G* level with different delocalizations are reported in Table 3. The $n_{X_1} \rightarrow \sigma^*_{X_2-Y}$ and $n_{X_2} \rightarrow \sigma^*_{X_1-Y}$ delocalizations tend to strengthen the X–X bond and the $E^{(2)}$ values increase in the order of X as S > Se > O. The $E^{(2)}$ values for X = O are considerably smaller due to high electroneativity and low polarizability of oxygen. The electron donating CH_3 substituent increases the $E^{(2)}$ energies in X = S and Se but no such effect is observed in case of X = O. Further increase in $E^{(2)}$ values is seen with π-donor $-NH_2$ substituent for X = S, Se. In addition the electron delocalization from lone pair present on N results in stabilization of the dichalcogenides and their transition states also. The NBO analysis clearly indicates that there is presence of partial π-character between S–S and Se–Se bonds. The additional $n_N \rightarrow \sigma^*_{X-X}$ electron delocalization however tends to weaken X–X bond and the same delocalization is responsible for stabilization of transition states in the order TS1 > TS2. The rotational barriers for H_2N–X–X–NH_2 are the net outcome of these electron delocalizations.

The NBO analysis suggests that π-character decreases in the order S > Se > O. The X–X barrier for rotation through TS2 represents the π-character more appropriately indicating that the π-character is larger in X = S than that in X = Se. Difference in rotational barriers for rotation through TS1 and TS2 of H_2X_2 molecules suggest the difference in repulsive interactions between the lone pairs and bond pairs in the two transition states. The higher O–O rotational barrier in dimethyl peroxide in comparison to C–C rotational barrier in *n*-butane results from the breaking of hydrogen bond interactions as indicated by nonbonded distance of 1.992 Å between (B3LYP/6-311++G**) oxygen and one of the hydrogens attached to methyl group.

The homolytic bond dissociation energy (BDE) is an important thermodynamic quantity measuring the strength of bonds as well as feasibility of formation and stability of radicals [40]. The BDEs of X–X bond in the molecules under study evaluated at B3LYP and MP2 theoretical levels using 6-311+G*, 6-311++G** and PVDZ basis sets are reported in Table 4. The values obtained at G2MP2 level are also included in the table. The X–H and C–X BDEs at B3LYP/6-311++G** and G2MP2 levels are listed in Table 5. The comparison of the values with experimental values suggest the good agreement between the theoretical and experimental results. The X–H BDEs are larger than X–X BDEs and the values decrease in the order of X as O > S > Se. Clearly, the X–H bond strength decreases with increase in size of the chalcogen.

The X–X BDE for X = Se, S, and O and Y = H are 55.12, 64.72, and 51.39 kcal/mol at G2MP2 level. The

Table 3
The second order energies $E^{(2)}$ (in kcal/mol) of dichalcogenides {chalcogen = [O], (S), Se} obtained by using NBO analysis at MP2/6-31+G* level

Molecule	Conformer	$n_{X1} \rightarrow \sigma^a_{X2-Y}$ X = Se, (S) [O] [a]Y = H, C, N	$n_{X2} \rightarrow \sigma^a_{X1-Y}$ X = Se, (S) [O] [a]Y = H, C, N	$n_{N3} \rightarrow \sigma^a_{X1-X2}$ X = Se, (S) [O] [a]Y = H, C, N	$n_{N4} \rightarrow \sigma^a_{X1-X2}$ X = Se, (S) [O] [a]Y = H, C, N
X_2H_2	GS	4.04 (4.86) [0.98]	4.04 (4.86) [0.98]	–	–
	TS1	–	–	–	–
	TS2	–	–	–	–
$X_2(CH_3)_2$	GS	5.82 (6.58) [0.82]	5.82 (6.58) [0.82]	–	–
	TS1	–	–	–	–
	TS2	–	–	–	–
$X_2(NH_2)_2$	GS	10.32 (11.29)	10.32 (11.29)	6.89 (8.34)	6.89 (8.34)
	TS1			13.53 (19.23)	13.57 (19.24)
	TS2	–	–	7.06 (9.65)	7.05 (9.64)

[a] Y, first atom of the substituent.

Table 4
Bond dissociation energies (in kcal/mol) of dichalcogenides {chalcogen = [O], (S),Se} at B3LYP (MP2) levels using 6-311+G*, 6-311++G**, and PVDZ basis set along with the experimental values available and the values at G2MP2 level

Molecule	6-311+G*	6-311++G**	PVDZ	G2MP2	Experimental[a,b]
HSe–SeH	51.9 (48.2)	51.5 (48.3)	51.1	55.1	–
$CH_3Se–SeCH_3$	48.9 (49.6)	48.9 (49.9)	48.7	56.9	–
$NH_2Se–SeNH_2$	31.3 (32.4)	31.6 (33.9)	32.0	36.1	–
HS–SH	55.1 (51.8)	54.7 (51.8)	57.2 (54.2)	64.7	66.0[a]
$CH_3S–SCH_3$	51.5 (54.6)	51.4 (55.1)	53.4 (57.7)	66.5	62 ± 2[a]
$NH_2S–SNH_2$	26.7 (28.6)	27.1 (29.6)	30.3 (34.0)	43.7	–
HO–OH	46.9 (47.8)	45.7 (46.9)	47.9 (49.3)	51.4	51.0[a]
$CH_3O–OCH_3$	28.6 (41.2)	28.4 (41.1)	48.3 (44.2)	42.3	35.9[b]

[a] See Ref. [22].
[b] See Ref. [50].

Table 5
Bond dissociation energies (in kcal/mol) of various molecules at B3LYP/6-311++G** and G2MP2 level

Molecule	6-311++G**	G2MP2	Experimental[a,b]
HOO–H	85.2	86.7	88.2 ± 1[a]
HSS–H	72.9	73.2	70.0 ± 1.5[a]
HSeSe–H	68.1	68.2	–
CH_3–OH	83.1	94.3	92.4[b]
CH_3–SH	65.8	75.8	74.7[b]
CH_3–SeH	59.1	67.2	–

[a] See Ref. [22].
[b] See Ref. [51].

experimental values [22] for O–O and S–S BDEs are 51.0 and 66.0 kcal/mol, respectively, that substantiates the reliability of G2MP2 results. The comparison of BDEs obtained at G2MP2 levels with the values obtained at other theoretical levels indicates that some of the BDE values obtained at B3LYP/6-311++G** level are close to G2MP2 values.

The X–X BDE energies for X_2H_2 decrease in the order S–S > Se–Se > O–O at all the theoretical levels. The H_3C-XH BDEs however decrease in the order O > S > Se at B3LYP/6-311++G** and G2MP2 level which indicates that increase in size of chalcogen leads to weakening of C–X bond. The X–X BDEs however do not show dependence on the size of the chalcogen. The BDE values and X–X rotational barriers clearly suggest that S–S bond is stronger than Se–Se and O–O bond which is also supported by NBO analysis. The methyl substituent increases X–X BDE while π-donor NH_2 decreases the X–X BDE in case of X = S, Se. The O–O BDE is decreased in the presence of CH_3 substituent. Negative hyperconjugative interactions stabilize the methyl substituted dichalcogenides while hyperconjugative interactions are important only in $CH_3O^{\cdot}$ as indicated by NBO analysis (Table 6).

The BDE data indicates that X–X bond strengths are determined by

(i) Hybridization and overlap of participating orbitals.
(ii) Replusive interactions between lone-pair lone-pair and bond-pair bond-pair.
(iii) Electron delocalization from lone pair of electrons present on X and the substituent.

4. Reactivity descriptors

Density functional theory makes use of electron density to derive different properties of molecules. The chemical potential (μ), electronegativity (χ), hardness (η) and softness (S) are parameters that correspond to linear responses of electron density with respect to changes in external potential and number of electrons [41,42]. The usefulness of these four parameters is related to hard-soft acid base principle [43]. The principle allowed the rationalization of a number of chemical interactions. Local descriptors like Fukui functions and local softness help in differentiating reactive behavior of atoms forming a molecule. The large f_{k+} and f_{k-}- values indicate high reactivity toward nucleophile and electrophile respectively [44].

The f_{k+} and f_{k-} values for O, S, and Se in X_2H_2 are reported in Table 7 The values indicate that higher chalco-

Table 6
Hyperconjugative and negative hyperconjugative interactions (in kcal/mol) in RX· radical (X = [O], (S), Se; R = CH_3, NH_2)

Radical	$n_{X1} \rightarrow \sigma_1^{a}{}_{Y–H}$ X = Se, (S), [O]	$n_{X1} \rightarrow \sigma_2^{a}{}_{Y–H}$ X = Se, (S), [O]	$n_{X2} \rightarrow \sigma_1^{a}{}_{Y–H}$ X = Se, (S), [O]	$n_{X2} \rightarrow \sigma_2^{a}{}_{Y–H}$ X = Se, (S), [O]
	Y = C, N	Y = C, N	Y = C, N	Y = C, N
$^{\cdot}XCH_3$	2.83 (3.81) [6.78]	3.71 (5.41) [6.68]	3.71 (3.81) [6.78]	2.83 (5.40) [6.68]
$^{\cdot}XNH_2$	1.20 (1.24)	1.20 (1.24)	2.92 (3.93)	2.92 (3.93)

[a] Y, first atom of the substituent.

Table 7
The Fukui functions and proton affinities (in kcal/mol) of O_2H_2, S_2H_2, Se_2H_2 at B3LYP/6-31+G* level

Molecule	f_{k+}	f_{k-}	PA
O_2H_2 (O)	0.389	0.411	161.44
S_2H_2 (S)	0.401	0.450	172.24
Se_2H_2 (Se)	0.403	0.449	179.50

gens X = S, Se both are better electrophile as well as better nucleophile in comparison to oxygen. The high nucleophilic character of S and Se reflects the easy availability of lone pairs of these chalcogens making them reactive enough and larger size of these helps in accepting electron density. The Fukui functions, however, do not help in distinguishing the electrophilic and nucleophilic character of sulfur and selenium. The proton affinities of H_2X_2 molecules increase in the order of X as O < S < Se which suggest that selenium is more nucleophilic.

5. Diselenides as glutathione peroxidase mimic

Few diselenide compounds have been tested for their ability to mimic glutathione peroxidase like catalytic activity. Glutathione peroxidase (GPx) is a well-known selenoenzyme that functions as an antioxidant [9,34,36,45–48]. The selenocysteine is present in the enzyme at the active site where selenium reduces hydrogen peroxides and organic peroxides. The selenol unit (Enzyme–SeH) is oxidized to selenenic acid (Enzyme–SeOH) which reacts with glutathione (GSH) to form selenyl sulfide adduct (Enzyme–SeSG). Active form of enzyme is regenerated by another glutathione that forms GSSG [34,36,45] (Fig. 1).

The free energy change for four steps in the catalytic cycle using diselenides as model compounds have been evaluated at B3LYP/6-311++G.

1. $RSeSeR + H_2O_2 \rightarrow RSeOOH + RSeH\ \Delta G1$
2. $RSeH + H_2O_2 \rightarrow RSeOH + H_2O\ \Delta G2$
3. $RSeOH + R'SH \rightarrow RSeSR' + H_2O\ \Delta G3$
4. $RSeSR' + R'SH \rightarrow RSeH + R'SSR'\ \Delta G4$

where R = NH_2, CH_3 and R′ = NH_2, CH_3.

The ΔG values for the reaction steps are given in Table 8. The free energy change for first three reaction steps have negative values indicating spontaneity of the reaction steps. The free energy change for the fourth reaction step is depicted to

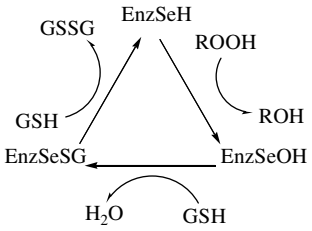

Fig. 1. Catalytic cycle of GPx.

Table 8
The free energy change in (kcal/mol) of various reaction steps (1–4) of substituted diselenides as model compounds at B3LYP/6-311++G level

Free energy change	NH_2	CH_3
$\Delta G1$	−7.35	−8.27
$\Delta G2$	−59.18	−49.43
$\Delta G3$	−19.79	−18.52
$\Delta G4$	2.98	4.05

be small and positive. The largest free energy change associated with the oxidation of selenol (RSeH) to selenenic acid (RSeOH) reflects the antioxidant ability of the selenium site; the electron-donating group further enhances this ability.

The experimental studies have been done by Mugesh et al. [34,45] on peroxidase like antioxidant activities of aryl diselenides having intramolecularly coordinating amino groups by characterizing the in situ intermediates by ^{77}Se NMR spectroscopy. From the difference in Se–N interactions, they suggested that the reactivity of selenenyl sulfide towards thiol determines the peroxidase activity of compounds. Musaev et al. [49] have shown that the reduction of selenyl sulfides to corresponding selenols is the rate determining step in the catalytic cycle of the GPx. The catalytic activity of selenium compounds against oxidative stress is due to its higher nucleophilicity and better reducing ability in comparison to lower chalcogen compounds.

6. Conclusions

In the present study, a number of theoretical methods have been employed to understand nature, strength and reactivity of dihydrogen dichalcogenides (chalcogen = O, S, Se) and their methyl and amino derivatives. The X–X rotational barriers through TS1 decrease in the order of X as O > S > Se. The barrier to rotation through TS2 is smaller than the values for similar rotation through TS1. The difference in the rotational barriers has been assigned to repulsive interactions of lone pairs and bond pairs in eclipsed orientation. The X–X BDE values decrease in the order S–S > Se–Se > O–O. The X–X BDE increase in dimethyl dichalcogenides while the values decrease in diaminodichalcogenides.

Appendix A. Supplementary data

Supplementary data associated with this article can be found, in the online version, at doi:10.1016/j.theochem.2007.01.038.

References

[1] G.I. Giles, C. Jacob, Biol. Chem. 383 (2002) 375.
[2] C. Jacob, W. Maret, B.L. Vallee, Proc. Natl. Acad. Sci. USA 96 (1999) 1910.
[3] K. Gato, M. Nagahama, T. Mizushima, K. Shimada, T. Kawashima, R. Okazaki, Org. Lett. 3 (2001) 3569.

[4] J.E. Spallholz, Biomed. Environ. Sci. 10 (1997) 260.
[5] H. Sies, Angew. Chem. Int. Ed. Engl. 25 (1986) 1058.
[6] L. Engman, D. stern, I.A. Cotgreave, C.M. Andersson, J. Am. Chem. Soc. 114 (1992) 9737.
[7] G.I. Giles, K.M. Tasker, R.J.K. Johnson, C. Jacob, C. Peers, K.N. Green, Chem. Commun. (2001) 2490.
[8] W.A. Pryor, Free Radicals in Biology, Academic Press, New York, 1976.
[9] T.G. Back, B.P. Dyck, J. Am. Chem. Soc. 119 (1997) 2079.
[10] T.G. Back, Z. Moussa, J. Am. Chem. Soc. 125 (2003) 13455.
[11] F. Tian, Z. YU, S. Lu, J. Org. Chem. 69 (2004) 4520.
[12] R. Benassi, F. Taddei, J. Phys. Chem. A 102 (1998) 6173.
[13] S. Carles, F. Lecomte, J.P. Schermann, C. Desfrancois, S. Xu, J.M. Nilles, K.H. Bowen, J. Berges, C.H. Levin, J. Phys. Chem. A 105 (2001) 5622.
[14] H. Nakamura, K. Nakamura, J. Yodoi, Annu. Rev. Immunol. 15 (1997) 351.
[15] G. Powis, J.R. Gaskada, M. Berggren, D.L. Kirkpatrick, L. Engman, I.A. Cotegreave, M. Angulo, A. Baker, Oncol. Res. 6 (1997) 303.
[16] A. Baker, C.M. Payne, M.M. Briehl, G. Powis, Cancer Res. 57 (1997) 5162.
[17] A. Gallegos, M. Berggren, J.R. Gaskada, G. Powis, Cancer Res. 57 (1997) 4965.
[18] H. Suzuki, K. Fukushi, S.I. Ikawa, S. Konaka, J. Mol. Struct. 221 (1990) 141, and references therein.
[19] W.J. Hehre, L. Radom, P.V.R. Schleyer, J.A. Pople, Ab initio Molecular Orbital Theory, Wiley, New York, 1986.
[20] R.G. Parr, W. Yong, Density-functional Theory of Atoms and Molecules, Oxford University Press, New York, 1989.
[21] M.J. Frish, G.W. Trucks, H.B. Schlegel, G.E. Scuseria, M.A. Robb, J.R. Cheeseman, V.G. Zakrzewski, J.A. Montgomery, R.E. Jr. Startmann, J.C. Burant, S. Dapprich, J.M. Milliam, A.D. Daniels, K.N. Kudin, M.C. Strain, O. Faraks, J. Tomasi, V. Barone, M. Cossi, R. Cammi, B. Mennucci, C. Pomelli, C. Adamo, S. Clifford, J. Ochterski, G.A. Peterson, P.Y. Ayala, Q. Cui, K. Morokuma, D.K. Malick, A.D. Rabuck, K. Raghavachari, J.B. Foresman, J. Cioslowski, J.V. Ortiz, A.G. Baboul, B.B. Stefanov, G. Liv, A. Liashenko, P. Piskorz, I. Komaromi, R. Gomperts, R.L. Martin, D.J. Fox, T. Keith, M.A. Al-Laham, C.Y. Peng, A. Nanayakkara, C. Gonzalez, M. Challacombe, P.M.W. Gill, B. Jonnson, W. Chen, M.W. Wong, J.L. Andres, C. Gonzalez, M. Head-Gordon, E.S. Replogle, J.A. Pople, GAUSSIAN 98, Revision A.7, Gaussian Inc., Pittsburgh, PA, 1998.
[22] D.F. McMillen, D.F. Golden, Annu. Rev. Phys. Chem. 33 (1982) 493.
[23] P. Burk, I.A. Koppel, A. Rummel, A. Trummal, J. Phys. Chem. A 104 (2000) 1602.
[24] A.K. Chandra, P.C. Nam, M.T. Nguyen, J. Phys. Chem. A 107 (2003) 9182.
[25] G.A. Dilabio, D.A. Pratt, A.D. Lofaro, J.S. Wright, J. Phys. Chem. A 103 (1999) 16502.
[26] A.K. Chandra, T. Uchimaru, Int. J. Mol. Sci. 3 (2002) 407.
[27] G.A. Dilabio, A.D. lofaro, J.S. Wright, J. Phys. Chem. A 103 (1999) 1653.
[28] D.A. Pratt, J.S. Wright, K.U. Ingold, J. Am. Chem. Soc. 121 (1999) 4877.
[29] P. Sinha, S.E. Boesch, C.G. Ralph, A. Wheeler, A.K. Wilson, J. Phys. Chem. A 108 (2004) 9213.
[30] D.A. Mcquarrie, Statistical Mechanics, Harper and Row, New York, 1976.
[31] A.P. Scott, L. Radom, J. Phys. Chem. 100 (1996) 16502.
[32] M.P. Andersson, P. Uvdal, J. Phys. Chem. A 109 (2005) 2937.
[33] A.E. Reed, L.A. Curtiss, F. Weinhold, Chem. Rev. 88 (1988) 899.
[34] G. Mugesh, A. Panda, H.B. Singh, N.S. Punekar, R.J. Butcher, J. Am. Chem. Soc. 123 (2001) 839, and references therein.
[35] T. Wirth, Molecules 3 (1998) 164.
[36] J.K. Pearson, R.J. Boyd, J. Phys. Chem. A 110 (2006) 8979.
[37] G. Mugesh, A. Panda, H.B. Singh, N.S. Punekar, R.J. Butcher, Chem. Commun. (1998) 2227.
[38] E. Herbst, G. Winnewisser, Chem. Phys. Lett. 155 (1989) 572.
[39] W.N. Hubbard, D.R. Douslin, C. Lee, J.P. Mccullaugh, D.W. Scott, S.S. Todd, J.F. Messerly, I.A. Hossenlopp, A. George, G. Waddington, J. Am. Chem. Soc. 80 (1958) 3547.
[40] E.I. Izgorodina, M.L. Coote, L. Radom, J. Phys. Chem. A 109 (2005) 7558.
[41] P. Fuentealba, P. Perez, R. Contreras, J. Chem. Phys. 113 (2000) 2544.
[42] D.J. Tozer, F.D. Proft, J. Phys. Chem. A 109 (2005) 8923.
[43] P. Perez, A.T. Lobbe, R. Contreras, J. Phys. Chem. A 104 (2000) 5882.
[44] P. Perez, A. Aizman, R. Contreras, J. Phys. Chem. A 106 (2002) 3964.
[45] B.K. Sarma, G. Mugesh, J. Am. Chem. Soc. 127 (2005) 11477.
[46] G. Mugesh, H.B. Singh, Chem. Soc. Rev. 29 (2000) 347.
[47] S.R. Wilson, P.A. Zucker, R.R.C. Huang, A. Spector, J. Am. Chem. Soc. 111 (1989) 5936.
[48] M. Iwaoka, S. Tomoda, J. Am. Chem. Soc. 116 (1994) 2557.
[49] R. Prabhakar, T. Vreven, K. Morokuma, D.G. Musaev, Biochemistry 44 (2005) 11864.
[50] J.A. Kerr, A.F. Trotman-Dickenson, Handbook of Chemistry and Physics, 50th ed., The Chemical Rubber Co., Cleveland, OH, 1969/70.
[51] L.A. Curtiss, K. Raghavachari, P.C. Redfern, J.A. Pople, J. Chem. Phys. 106 (1997) 1063.